Performance of Fuzzy C-Means Algorithm on Leukocyte Image Segmentation

Khakim Assidiqi Nur Hudaya[1], Budi Sunarko[2], Anan Nugroho[3*]

***Abstract*— Image segmentation is one of the most critical steps in computer-aided diagnosis that potentially accelerate leukemia diagnosis. Leukemia is categorized as blood cancer known as a deadly disease. Generally, acute lymphoblastic leukemia (ALL) detection can be done manually by counting the leukocytes contained in the stained peripheral blood smear image using the immunohistochemical (IHC) method. Unfortunately, the manual diagnosis process takes 3−24 hours to complete and is most likely inaccurate due to operator fatigue. An image segmentation method proposed by Vogado can achieve an accuracy of 98.5%. However, this method uses a K-means clustering algorithm that is not optimal for input images containing mostly noise. In this research, fuzzy c-means were applied to solve this problem. The dataset used in this study was ALL-IDB2, which consisted of 260 images, with each image having the size of 257×257 pixels in tagged image file (TIF) format. The initial stage of this method was to divide the ALL-IDB 2 acute leukemia dataset image into cyan, magenta, yellow, key (CMYK) and L*a*b color schemes which then subtract the M component subtracted by component *b. The subtraction results were then splits using the FCM algorithm, resulting in the nucleus and background sections. The output of this method was then evaluated and measured using the metrics accuracy, specificity, sensitivity, kappa index, dice coefficient, and time complexity. The results showed that changing the clustering algorithm in the image segmentation method did not provide a significant change in results; an increase occurred in the specificity and precision metrics with an average of 0.1−0.4%, the execution time also increased by an average of 23.10%. The decrease in the accuracy metric was down to 95.4238%, and the dice coefficient value was 79.3682%. From the explanation above, it can be concluded that the application of the FCM algorithm to the segmentation method does not provide optimal results.**

***Keywords*—Image Segmentation, Clustering, Leukemia, K-Means, Fuzzy C-Means.**

I. INTRODUCTION

Leukemia is one of the deadly diseases categorized as blood cancer [1]. Leukemia occupies the 8th position for the number of incidents and ranks 9th for the number of deaths at the world level. [2]. Generally, acute lymphoblastic leukemia (ALL) detection is conducted manually in the hospital by counting the leukocytes found in the stained peripheral blood smear image using the immunohistochemical (IHC) method. Unfortunately, the manual diagnosis process takes 3−24 hours until the results come out [3]. Currently, there is a computer-aided diagnosis (CAD) that can diagnose leukemia within 5−15 minutes with an accuracy of up to 97% [4], [5].

Segmentation is the essential part of the automatic diagnosis system for ALL. Reference [1] proposed an automatic leukocyte segmentation method that succeeded in getting the second-best outcome assessment out of fifteen methods tested in a study on four different datasets [6]. This method converted color images into cyan, magenta, yellow, key (CMYK) and L*a*b color schemes. Then, a contrast adjustment was applied to the M component from the CMYK color scheme and *b from the L*a*b color scheme, followed by a 7×7 median filter to remove the noise in the image. Next, the *b component was reduced by the M component to obtain a contrasting leukocyte image. This image was used as input to the k-means (KM) clustering algorithm, dividing it into three parts: the nucleus, cytoplasm, and background. Light colors (near white) were classified as the nucleus, while darker colors were categorized as cytoplasm and background. Finally, morphological operations (dilation and erosion) were applied to reduce noise in the previous stage.

A grouping-based technique is a technique commonly used to separate data into several clusters that have similar characteristics. KM grouping is a partitioned grouping technique in which each cluster is created with the help of the centroid. It becomes the most typically used iteration technique due to its ease of implementation. Although it is simple and frequently used, unfortunately, this technique has some drawbacks. For instance, the value of *k* must be determined in advance, otherwise it will potentially lose small groups. In addition, KM is not reliable in handling noise [7]. Several experiments have been conducted to improve the efficiency of the KM algorithm, such as a modified version of KM called moving k-means (MKM) which aims to maintain the uniformity of each cluster's endurance value so that clusters with low endurance values will not be grouped with high endurance value clusters [8]. Then, the enhanced moving k-means (EMKM) algorithm is proposed to improve KM performance, especially to avoid the central point trapped in the optimum local location [9]. Although it has been immensely improved, the EMKM algorithm is still based on the KM algorithm, which is less reliable in dealing with noise. A fuzzy logic-based clustering algorithm is proposed under fuzzy c-means (FCM) [10]. In FCM, each point has a degree of membership for all clusters. Each cluster is essential for each point, judged by its membership degree. In [9], the FCM clustering algorithm was superior to KM in the mean square error (MSE) measurement metric on five different test images. FCM obtained an MSE score of 314,432 in which better than KM with 320,731.

[1,2,3] *Electrical Engineering Department, Universitas Negeri Semarang, Jl.Taman Siswa, Sekaran, Kota Semarang, INDONESIA 50229 (phone: 024-8508093); e-mail:* [1]*khakim.a@students.unnes.ac.id,* [2]*budi.sunarko@mail.unnes.ac.id,* [3]*anannugroho@mail.unnes.ac.id)*

[*] *Corresponding Author*

[Received: 22 November 2021, Revised: 4 January 2022]

Until this paper was written, several studies have been conducted on image segmentation using clustering or morphological methods. KM grouping was applied to the L*a*b color scheme image to separate leukocytes and classify the image into four types of leukemia [11]. Preprocessing was done to convert the red, green, blue (RGB) image to the L*a*b color scheme. Subsequently, the KM clustering algorithm was applied to segment the image into three groups, namely the nucleus, background, and several other elements, such as cytoplasm and red blood cells. The group with the most blue color was determined as the nucleus.

Reference [1] converted color images to CMYK and L*a*b color schemes. After that, a contrast adjustment was applied to the M components of the CMYK color scheme and *b from the L*a*b color scheme. A 7×7 median filter was also applied to eliminate noise. Next, the *b component was reduced by the M component. This process aimed to obtain a contrasting leukocyte image. This image was used as input to the KM algorithm, dividing the image into three parts, namely the nucleus, cytoplasm, and background. A light color (close to white) was classified as a nucleus. Finally, morphological operations (dilation and erosion) were applied to reduce noise in the previous stage.

Another study applied a median filter followed by masking to reduce the sharpness of the image. Then, the image color scheme was changed from RGB to L*a*b [12]. Next, the segmentation step was conducted in two stages. The first segmentation was attained by an improved version of the fuzzy-clustering technique, namely the Gustafson-Kessel grouping, then classifying the closest neighbors in the L*a*b* space.

In [13], the Otsu thresholding segmentation method generated a binary image to separate red blood cells and malaria parasites. The method succeeded in achieving 94.60% accuracy in classification. Although the result was reasonably good, some segmentation errors occurred. These errors were caused by the loss of vital information during the conversion process into a grayscale image.

II. METHODOLOGY

A. Study Area and Data

The dataset used in this paper was ALL-IDB2 secondary data, which was a categorized ALL-IDB dataset. Fig. 1 shows the image of the ALL-IDB dataset. The image was taken using a PowerShot G5 camera with 2,592×1,944 resolution in JPG format. Several data that were labeled by experts amounted to 260 images which size was 257×257 pixels each in TIF format. This data, published by the Faculty of Information Technology Università Degli Studi in Milano, taken from the S. Gerardo Hospital, Monza, Italy, was then classified by Prof. Andrea Biondi and Dr. Oscar Maglia of The Tettamanti Research Center.

B. Image Preprocess

The proposed method contains a flow chart that are divided into three main stages, as shown in Fig. 2. First, the program converts color images into CMYK and L*a*b color schemes. Then, a contrast adjustment is applied to the M component from the CMYK color scheme and *b from the L*a*b color scheme, followed by using a 7×7 median filter to remove noise from the input image. Furthermore, the *b component is reduced by the M component to obtain a contrasting leukocyte image. This image is used as an input to the FCM algorithm.

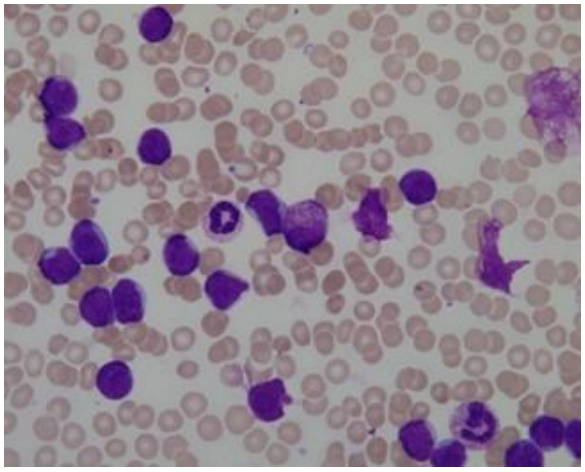

Fig. 1 ALL-IDB dataset image.

C. Clustering

Simply put, the FCM algorithm was began by determining the number of clusters to use, then randomly assigned each pixel data into several clusters. Subsequently, the centroid point was determined again using (1) until certain conditions were met. The clustering algorithm's output was data divided into three parts, namely the nucleus, cytoplasm, and background. The image resulting from the clustering algorithm would generate a binary image with a value range of 0 to 255. The light color was represented by a value of 255, and the dark color was represented by 0. The cluster with the highest color range or the lightest color was classified as a nucleus. The nucleus part would be stored in a new variable and continued in the post-processing stage.

D. Post Image Processing

At this stage, morphological operations were caried out to reduce noise in the previous stage. This operation included dilation, with a masking value of 7 pixels in a disc form, and erosion, with a masking value of 3 pixels in a ball form.

E. Data Analysis Technique

The data analysis technique used was an overlap validation measurement. It compares two image segmentation results by measuring the relationship and similarity between the two. When one image is reviewed for its performance, the other is the expected result, or it could be called ground truth (GT). This evaluation applied quantitative analysis to measure the performance of an algorithm without affected by human error factors, considering that the analysis was conducted automatically by comparing the GT of each pixel. The metrics used in this paper were accuracy (A), specificity (S), precision (P), recall (R), dice-coefficient (DC), and kappa index (K). Measurement was initiated by comparing each pixel in the segmented image, as shown in Fig. 3(a), with the GT image is

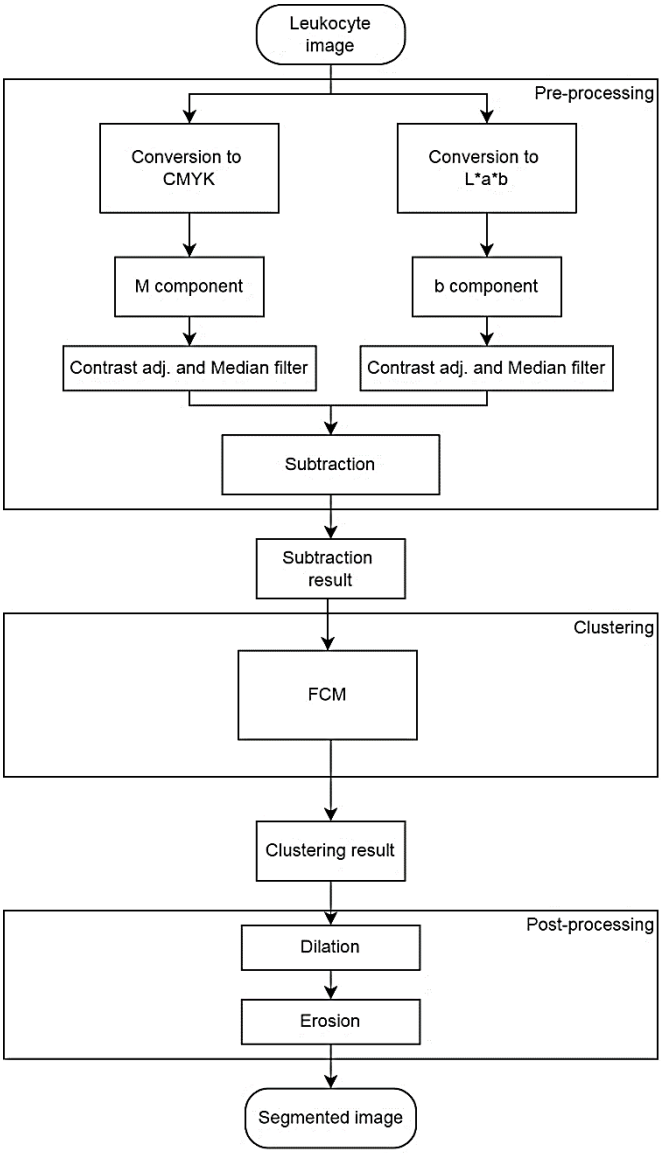

Fig. 2 Flowchart of the proposed method.

shown in Fig. 3(b). When the pixel value of the image segmentation was the same as GT, the pixel was categorized as a true positive (TP) or the correct result. On the other hand, if each segmented pixel was not equal to GT, then the pixel was categorized as false positive (FP) or false negative (FN), as shown in Fig. 4 [14].

A defines the number of positive and negative pixels that are successfully grouped divided by all values being studied. Then, the value is formulated in (1).

$$A = \frac{TP+TN}{TP+FN+TN+FP}. \quad (1)$$

S represents the percentage of pixels successfully determined as negative divided by the number of positive samples. The process can be expressed by (2). Looking at the leukemia diagnosis scale, the value of *S* indicates that this segmentation method will be sensitive to data that is not affected by leukemia.

$$S = \frac{TN}{TN+FP}. \quad (2)$$

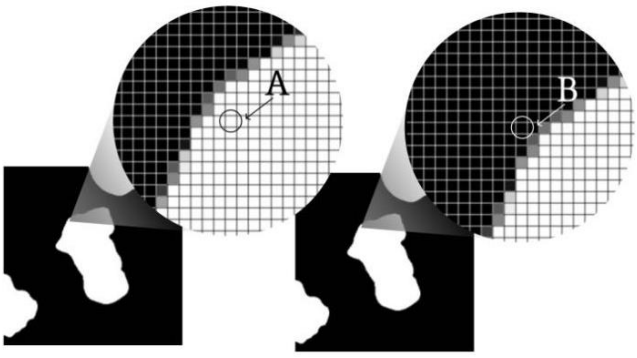

(a) (b)

Fig. 3 Comparison of ground truth and segmented images, (a) segmented images, (b) ground truth.

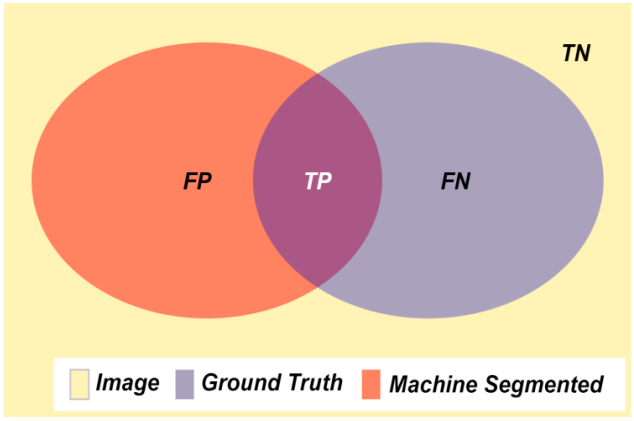

Fig. 4 Section diagram of TP, TN, FP, and FN.

P and *R* measurements represent the similarity in the number of pixels that are segmented automatically and the GT reference image. *P* reflects the proportion between TP results and their relationship to all positive predictions, as shown in (3). In contrast, the *R* is the division of TP by the summation of FN and TP, as in (4).

$$P = \frac{TP}{TP+FP} \quad (3)$$

$$R = \frac{TP}{TP+FN}. \quad (4)$$

The DC is used to verify whether the leukocytes are segmented correctly. For each segmented leukocyte, DC is calculated using (5).

$$DC = \frac{2\times TP}{2\times(TP+FP+FN)}. \quad (5)$$

Another metric used was the kappa index (*K*), which reflects the value in the confusion matrix.

$$K = \frac{\theta_1-\theta_2}{1-\theta_2} \quad (6)$$

with θ_1 is expressed in (7) and θ_2 in (8).

$$\theta_1 = \frac{TP+TN}{TP+TN+FP+FN} \quad (7)$$

$$\theta_2 = \frac{((TP+FN)*(TP+FP))+((TN+FN)*(TN+FP))}{(TP+TN+FP+FN)^2}. \quad (8)$$

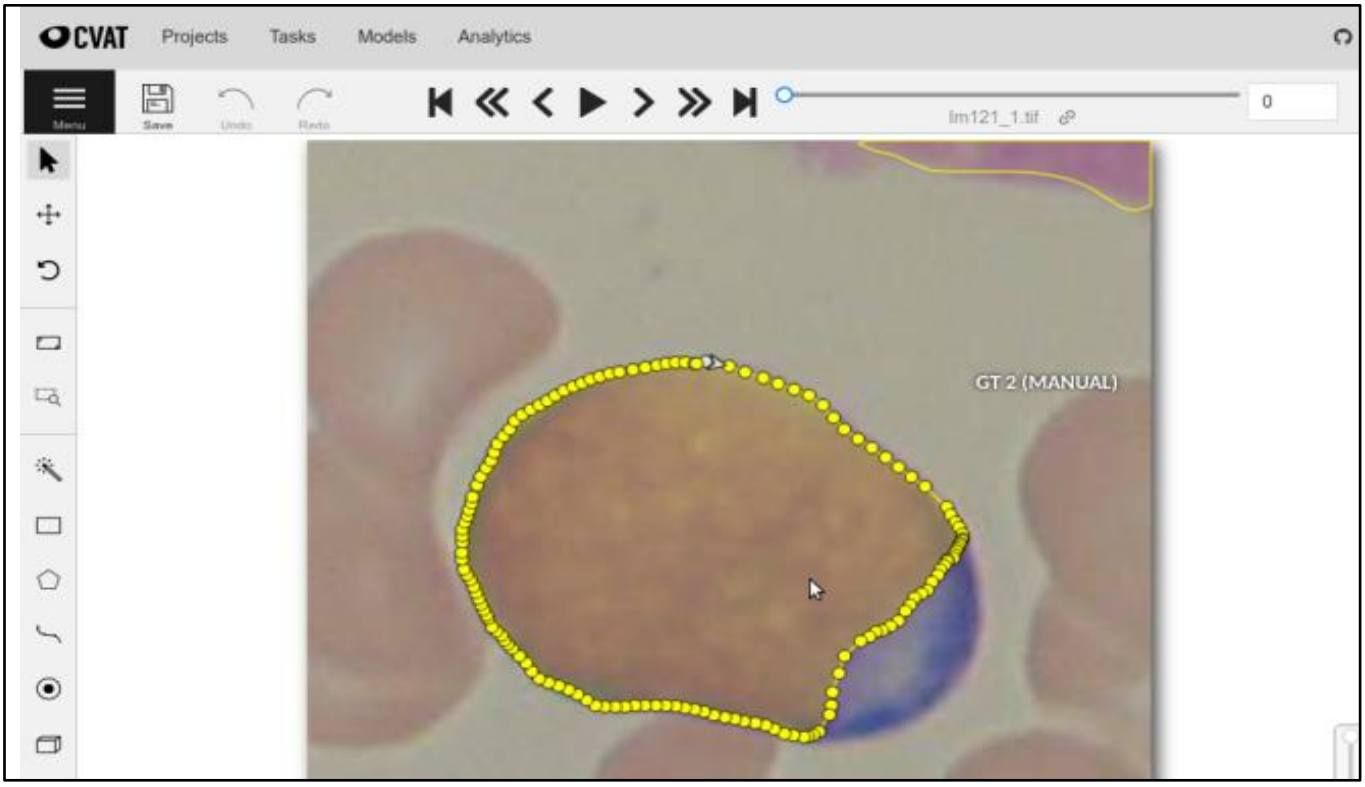

Fig. 5 The process of making ground truth using CVAT.

The value scales of the *A*, *S*, *P*, *R*, *DC*, and *K* measurement metrics were standardized to a percent, or between 0 and 100. Finally, the time complexity (*T*) metric adopted the commonly used time unit, the second.

F. Testing

Python programming language version 3.6.9 was used to write the image segmentation algorithm into a computer program. The Google Colab software was used to write programs (coding) accessed through the Google Chrome web browser version 76 installed on the Microsoft Windows 7 64 bit operating system. This image segmentation program required several additional libraries, such as Open CV version 4.1.0, Numpy version 1.16.3, Sklearn version 0.16.0, and Fuzzy-c-means version 1.2.4. The program was run on Google Colab, a virtual machine with standard specifications of two vCPUs with a speed of 2.2 GHz each and RAM with a capacity of 13 GB. The execution results were then compared with the source segmentation method [1], written in C language and used in MATLAB. The research was conducted through image analysis from the program output and the original diagnosis by an expert determined in GT in the ALL-IDB2 dataset. As in Fig. 5, GT was created using the Computer Vision Annotation Tool (CVAT) program.

III. Results and Discussion

After the program was run on 260 images, one sample image was taken to be analyzed in more detail. Fig. 6(a) is the original dataset image processed by both methods. Next, Fig. 6(b) displays the M component image of the original image converted to the CMYK color scheme. Fig. 6(c) is a component *b of the original image converted into the CIELAB color scheme; Fig. 6(d) is the image after applying the contrast adjustment and median filter to the M component. Fig. 6(e) is the image after applying the contrast adjustment and median filter to component *b. Fig. 6(f) shows the result of subtraction between components *b and M. After that, Fig. 6(g) is the image after undergoing FCM algorithm processing while Fig. 6(h) is the final result of the proposed segmentation method.

The value of the method execution results in [1] and the results of the composition method are presented in Table I. The evaluation result values of the leukocyte image were obtained by recording the execution results of each image, followed by calculating the average of all the leukocyte images tested.

In the *S* and *P* measurement metrics, the proposed composition method was superior to the original method with values of 98.79% and 94.41%, respectively. The increase in the value of *S* indicates that the composition method has better results in segmenting only the background (TN) part. Meanwhile, the increase in the *P* value reflects the proportional relationship between the actual detected pixel value (TP) and another positive pixel value (TP + FP). The analysis also showed a decrease in several other metrics, namely *A*, *R*, *DC*, and *K*. Technically, a decrease in accuracy means a decrease in the number of overlapping pixels matches between the auto segmentation results and GT, or conversely, more parts on the automatic segmentation results are not as expected.

Several factors led to the decrease in value, namely, the FCM clustering algorithm lied in the part between preprocessing and morphological operations. It indicates that the input grouping

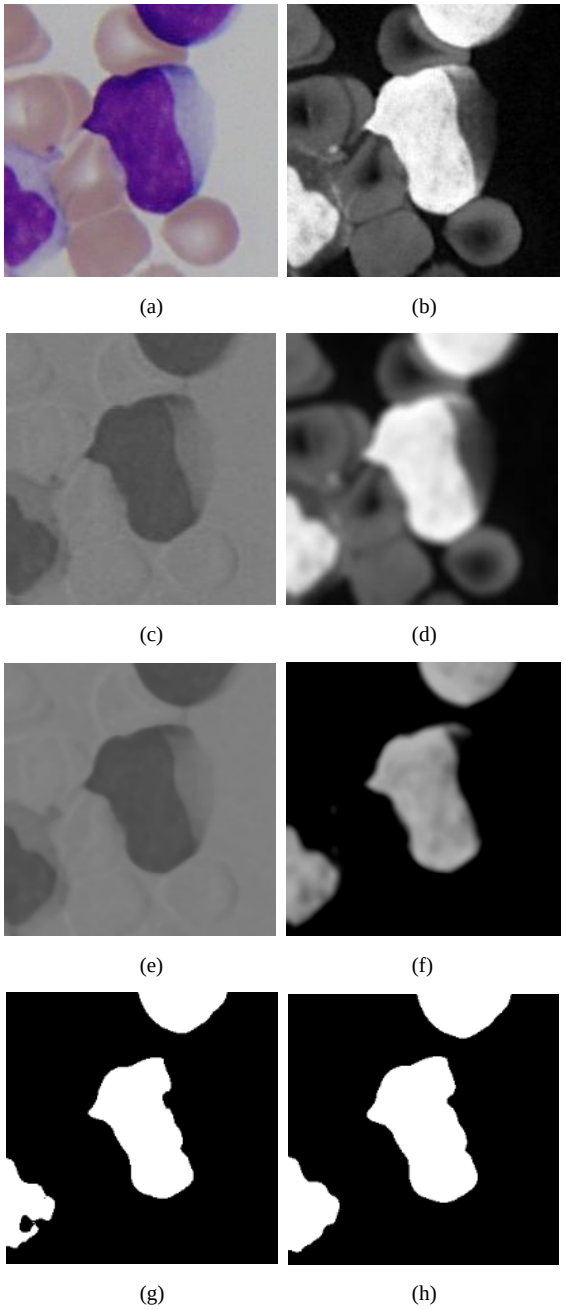

Fig. 6 Image comparison, (a) original image, (b) M component from CMYK, (c) component *b from CIELAB, (d) application of contrast adjustment and median filter to M component, (e) application of contrast adjustment and median filter on component *b, (f) the result of subtraction between b* - M, (g) the result of FCM clustering, (h) the final result of segmentation.

data had undergone simplification in reduction, color separation, and median filter so that the noise tends to have been eliminated, as shown in Fig. 6(f). It is related to the finding that FCM is more reliable in dealing with noise [15]. In the method in [1], the image has already been processed and reduced to only one-color channel (grayscale). Thus, determining the centroid point using fuzzy calculations was not very effective and tended to prolong the execution time of an algorithm.

TABLE I
ALGORITHM EFFECTIVENESS ON THE ALL-IDB2 DATASET

Metric	Method in [1]	Composed Method
A (%)	95.4238	95.1645
S (%)	98.6772	98.7880
P (%)	94.0286	94.4084
R (%)	83.4178	81.7165
K (%)	85.3030	84.3539
DC (%)	79.3682	78.1263
T (s)	3.5753	4.3287

The results also showed that the operating time of the method increased by an average of 23.10% or between 0.5−0.8 seconds. It was because FCM is an algorithm based on cryptic iteration calculations, so not only can each object have one cluster, but it can also have many clusters with varying degrees of membership. Based on (9), the FCM algorithm requires an additional step to calculate the weight of each element (*w*) anytime an iteration is performed. That is why FCM requires a longer processing time than KM.

$$J = \sum_{i=1}^{n} \sum_{j=1}^{c} w_{ij}^{m} \left\| x_i - c_j \right\|^2. \quad (9)$$

For example, in KM, each object only has cluster ownership between 1 or 0. However, in FCM, it can be between 1 and 0. This multiple cluster ownership certainly affects the number of iterations, allowing increase in the computation time. The more iterations, the longer it will take. This finding is in line with previous studies [15].

Although there was a decrease, the change in value was not too significant. The average change only ranged from 0.01% to 0.61%, and the time changed only 0.5−0.8 seconds. However, the change in time was significant enough to affect the relatively high image resolution of the tested data.

IV. CONCLUSION

In this paper, an attempt has been made to analyze the impact of performance changes on image segmentation of white blood leukemia. Changing the KM clustering algorithm to FCM was applied to the segmentation method of previous studies. This method was tested using 260 images in the ALL-IDB2 dataset. The analysis was conducted from six measurement metrics: accuracy, specificity, precision, recall, dice-coefficient, and kappa index. After the testing, results showed there was an increase in specificity and precision metric values as well as a decrease in other metrics. Hence, it can be concluded that there is a decrease in performance as the input data of the clustering method has undergone simplification in the form of reduction and median filter (at the preprocessing stage), indicating that noise tends to have been eliminated. In addition, the use of the FCM algorithm prolonged the program execution time (time complexity). Therefore, the application of the FCM algorithm to the segmentation method of previous studies did not provide optimal results. Further research can be done to analyze the effect of converting into KM algorithms that have been refined, such as EMKM. Moreover, testing on different data sets can also be a theme for further research.

CONFLICTS OF INTEREST

During the writing and conduction of this research, authors declare no conflicts of interest with any parties. All information delivered is the actual result obtained from conducting research and is not influenced by personal opinion or interest.

AUTHOR CONTRIBUTIONS

This research is collaborative research conducted by three authors. The followings are the distribution of the authors' contribution to this research. Conceptualization, Khakim Assidiqi Nur Hudaya and Budi Sunarko; writing—original draft and administration preparation, Khakim Assidiqi Nur Hudaya and Anan Nugroho; software and data collection, Khakim Assidiqi Nur Hudaya; supervision and validation, Budi Sunarko.

REFERENCES

[1] L.H.S. Vogado, R.M.S. Veras, F.H.D. Araujo, R.R.V. Silva, and K.R.T. Aires, "Leukemia Diagnosis in Blood Slides Using Transfer Learning in CNNs and SVM for Classification," *J. Eng. Appl. Artif. Intell.*, Vol. 72, pp. 415–422, Jun. 2018.

[2] (2021) American Cancer Society website, [Online], https://www.lls.org/facts-and-statistics/facts-and-statistics-overview/facts-and-statistics, access date: 2-May-2021.

[3] I. Naz, N. Muhammad, M. Yasmin, M. Sharif, J.H. Shah, and S.L. Fernandes, "Robust Discrimination of Leukocytes Protuberant Types for Early Diagnosis of Leukemia," *J. Mech. Med. Biol.*, Vol. 19, No. 6, pp. 1-17, 2019.

[4] E.W. Abdulhay, M.A. Mohammed, D.A. Ibrahim, N. Arunkumar, and V. Venkatraman, "Computer Aided Solution for Automatic Segmenting and Measurements of Blood Leucocytes Using Static Microscope Images," *J. Med. Syst.*, Vol. 42, No. 4, pp. 1-12, 2018.

[5] A. Nugroho, R. Hidayat, and H.A. Nugroho, "Thyroid Ultrasound Image Segmentation: A Review," *IEEE 5th Int. Conf. Sci. Technol. (ICST)*, 2019, pp. 1-6.

[6] A.R. Andrade, L.H.S. Vogado, R. de M.S. Veras, R.R.V. Silva, F.H.D. Araujo, and F.N.S. Medeiros, "Recent Computational Methods for White Blood Cell Nuclei Segmentation: A Comparative Study," *Comput. Methods Programs in Biomed.*, Vol. 173, pp. 1–14, 2019.

[7] M. Ahmed, R. Seraj, and S.M.S. Islam, "The K-Means Algorithm: A Comprehensive Survey and Performance Evaluation," *Electron.*, Vol. 9, No. 8, pp. 1-12, 2020.

[8] M.Y. Mashor, "Hybrid Training Algorithm for RBF Network," *Int. J. Comput., Internet, Manage.*, Vol. 8, No. 2, pp. 50-65, 2000.

[9] F.U. Siddiqui and N.A.M. Isa, "Enhanced Moving K-Means (EMKM) Algorithm for Image Segmentation," *IEEE Trans. Consum. Electron.*, Vol. 57, No. 2, pp. 833–841, 2011.

[10] J.C. Dunn, "A Fuzzy Relative of the ISODATA Process and Its Use in Detecting Compact Well-Separated Clusters," *J. Cybern.*, Vol. 3, No. 3, pp. 32-57, 1973.

[11] S. Agaian, M. Madhukar, and A.T. Chronopoulos, "Automated Screening System for Acute Myelogenous Leukemia Detection in Blood Microscopic Images," *IEEE Syst. J.*, Vol. 8, No. 3, pp. 995-1004, 2014.

[12] S. Mohapatra, D. Patra, S. Kumar, and S. Satpathy, "Lymphocyte Image Segmentation Using Functional Link Neural Architecture for Acute Leukemia Detection," *Biomed. Eng. Lett.*, Vol. 2, No. 2, pp. 100-110, 2012.

[13] B. Sunarko, Djuniadi, M. Bottema, N. Iksan, K.A.N. Hudaya, and M.S. Hanif, "Red Blood Cell Classification on Thin Blood Smear Images for Malaria Diagnosis," *J. Phys.: Conf. Ser.*, Vol. 1444, pp. 1-8, 2020.

[14] A. Nugroho, R. Hidayat, H.A. Nugroho, and J. Debayle, "Ultrasound Object Detection Using Morphological Region-based Active Contour: An Application System," *Int. J. Innov. Learn. (IJIL)*, Vol. 29, No. 4, pp. 412-430, 2021.

[15] D.J. Bora, "Performance Comparison of K-Means Algorithm and FCM Algorithm with Respect to Color Image Segmentation," *Int. J. Emerg. Technol., Adv. Eng.*, Vol. 7, No. 8, pp. 460-470, 2017.